Proceedings of IMECE2009
2009 ASME International Mechanical Engineering Congress and Exposition
November 13-19, Lake Buena Vista, Florida, USA

IMECE2009-12342

MODELING OF ULTRAFAST PHASE CHANGE PROCESSES IN A THIN METAL FILM IRRADIATED BY FEMTOSECOND LASER PULSE TRAINS

Jing Huang, Yuwen Zhang[1,2,3], and J.K. Chen[2,3]
Department of Mechanical and Aerospace Engineering
University of Missouri
Columbia MO 65211, USA

Mo Yang[3]
College of Energy and Power Engineering
University of Shanghai for Science and Technology
Shanghai 200093, China

ABSTRACT

Ultrashort laser pulses can be generated in the form of a pulse train. In this paper, the ultrafast phase change processes of a 1-μm free-standing gold film irradiated by femtosecond laser pulse trains are simulated numerically. A two-temperature model coupled with interface tracking method is developed to describe the ultrafast melting, vaporization and resolidification processes. To deal with the large span in time scale, variable time steps are adopted. A laser pulse train consists of several pulse bursts with a repetition rate of 0.5~1 MHz. Each pulse burst contains 3~10 pulses with an interval of 50 ps ~ 10 ns. The simulation results show that with such a configuration, to achieve the same melting depth, the maximum temperature in the film decreases significantly in comparison to that of a single pulse. Although the total energy depositing on the film will be lifted, more energy will be transferred into the deeper part, instead of accumulating in the sub-surface layer. This leads to lower temperature and temperature gradient, which is favorable in laser sintering and laser machining.

INTRODUCTION

Because of its unique characteristics in material processing, fast fabrication and diagnostic, the interaction between ultrashort pulse lasers, especially femtosecond lasers, with metals has received a lot of research attentions in the past two decades. Various computational models were put forward and developed to describe the non-equilibrium energy transport phenomena during the process. One of the classical methods is the two-temperature model, which was originally proposed by Anisimov [1] and then rigorously derived by Qiu and Tien [2] based on the Boltzmann equation. The nonequilibrium energy transport between electron and lattice can also be described by the dual-phase-lag model [3, 4]. Jiang and Tsai extended the existing two-temperature model to high electron temperatures by using full-run quantum treatments [5]. Chen et al. proposed a semiclassical two-step heating model to investigate thermal transport in metals caused by ultrashort laser irradiation [6].

Ultrashort laser pulses can be generated by a mode-locked laser in the form of pulse train. With the rapid development of modern laser technology, currently the laser pulses are highly controllable with a wide range of parameters. A pulse train consists of a certain number of laser bursts launched at a fixed repetition rate f_{rep}, usually at the order of 10^3~10^6 Hz. Each burst can be composed of several consecutive femto- to picosecond laser pulses with a separation time (t_{sep}) of 100 femtoseconds to thousands of picoseconds. However, in most existing theoretical works, only the heating of thin films by a single femtosecond pulse was studied [7-13]. While these works provided basic understanding on the mechanism of interaction between ultrashort pulses and metals, there is still some distance between the physical models and real applications. Jiang and Tsai [14] studied the laser heating of gold thin films by femtosecond pulse trains, the effects of repetition rate and pulse separation were studied. Phase change

[1] Corresponding author. zhangyu@missouri.edu
[2] Fellow ASME
[3] Professor

was not considered in their model since the lattice temperature was well below melting point of gold. The same group also carried out research on the interaction of laser pulse trains with dielectrics [5, 15].

Most existing two-temperature model dealt with the case that lattice temperature is well below the melting point and only pure conduction is considered. Under higher laser fluence and/or short pulse, the lattice temperature can exceed the melting point and melting takes place [16]. At even higher laser fluence, the liquid surface temperature may exceed the saturation temperature and evaporation may occur. Both melting and evaporation processes were considered and integrated into the simulation in Ref. [17] and [18]. Chen and Beraun [19] proposed a computational model which considered the superheating and material ablation and studied the ablation depth caused by two consecutive pulses split from a laser beam. Huang et al. [18] studied the phase change of gold thin film during the irradiation of multiple femtosecond laser pulses. The relationship between the maximum vaporization temperature and melting depth, ablation depth were analyzed and compared with those of the sing pulse irradiation.

In this paper, based on the two-temperature model, the interface tracking methods is coupled to delineate the phase change processes during the interaction of femtosecond laser pulse trains and thin gold film. To conquer the large time-scale involved in the problem, variable time steps are used to control the computation time. The effects of repetition frequency, separation time between pulses and pulses number per train on the phase change processes are investigated.

NOMENCLATURE

Be	coefficient for electron heat capacity (J/m^3-K^2)
C	heat capacity (J/m^3-K)
c_p	specific heat (J/kg-K)
f_{rep}	repetition rate (Hz)
G	electron-lattice coupling coefficient (W/m^3-K)
h	latent heat of phase change (J/kg)
J_i	single pulse fluence (J/cm^2)
J_t	total energy of a pulse train (J/cm^2)
k	thermal conductivity (W/m-K)
L	thickness of the metal film (m)
M	molar mass (kg/kmol)
q''	heat flux (W/m^2)
R	reflectivity
R_g	specific gas constant (J/kg-K)
R_u	universal gas constant (J/kmol-K)
s	interfacial location (m)
S	intensity of the internal heat source (W/m^3)
t	time (s)
t_p	pulse width (s)
t_{sep}	separation time (s)
T	temperature (K)
T_F	Fermi temperature (K)
T_m	melting point (K)
u	interfacial velocity (m/s)
V_0	interfacial velocity factor (m/s)
x	coordinate (m)
Greek Symbols	
δ	optical penetration depth (m)
δ_b	ballistic range (m)
ε	total emissivity
ρ	density (kg/m^3)
σ	Stefan–Boltzmann constant (W/m^2-K^4)
Superscripts	
0	last time step
Subscripts	
0	initial condition
e	electron
i	pulse sequence
l	lattice
ℓ	liquid
R	thermal radiation
s	solid
$s\ell$	solid-liquid interface
sur	surface
∞	ambient environment

PHYSICAL MODEL

Figure 1 shows the physical model of the problem under consideration. A laser pulse train impinges on the right side of a free standing gold film, which has a thickness of L. The thickness is very small in comparison to the radius of the laser beam; therefore this problem can be approximated to be one-dimensional. Figure 2 shows the structure of a laser pulse train. As stated above, f_{rep} and t_{sep} are the repetition rate and separation time respectively. Each single pulse is assumed to be temporally Gaussian. The pulse duration (t_p), defined as the full width at half maximum (FWHM), is fixed to be 100 fs in the current work.

The two-step heating model for free electrons and the lattice are given by [20]

$$C_e \frac{\partial T_e}{\partial t} = \frac{\partial}{\partial x}\left(k_e \frac{\partial T_e}{dx} \right) - G(T_e - T_l) + S \tag{1}$$

$$C_l \frac{\partial T_l}{\partial t} = \frac{\partial}{\partial x}\left(k_l \frac{\partial T_l}{dx} \right) + G(T_e - T_l) \tag{2}$$

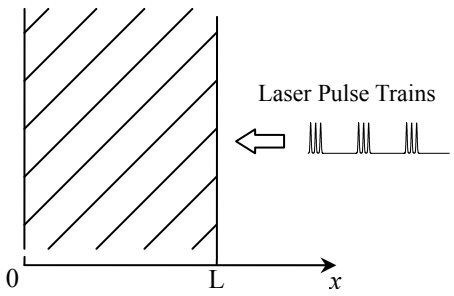

Fig. 1 Laser irradiation on thin film

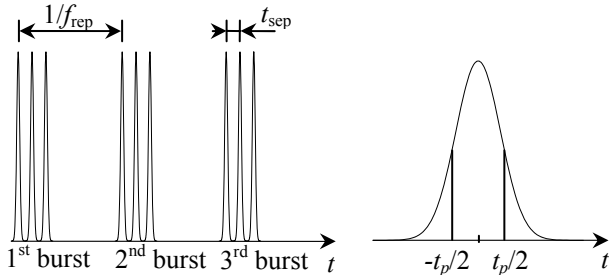

Fig. 2 Laser pulse train

The heat capacity of electron C_e, as suggest by Chen et al. [6], is approximated by

$$C_e = \begin{cases} B_e T_e, & T_e < T_F/\pi^2 \\ 2B_e T_e/3 + C_e'/3, & T_F/\pi^2 \le T_e < 3T_F/\pi^2 \\ Nk_B + C_e'/3, & 3T_F/\pi^2 \le T_e < T_F \\ 3Nk_B/2, & T_e \ge T_F \end{cases} \quad (3)$$

where

$$C_e' = B_e T_F/\pi^2 + \frac{3Nk_B/2 - B_e T_F/\pi^2}{T_F - T_F/\pi^2}\left(T_e - T_F/\pi^2\right) \quad (4)$$

The thermal conductivity of electron k_e can be obtained by [21]

$$k_e = \chi \frac{\left(\vartheta_e^2 + 0.16\right)^{5/4}\left(\vartheta_e^2 + 0.44\right)\vartheta_e}{\left(\vartheta_e^2 + 0.092\right)^{1/2}\left(\vartheta_e^2 + \eta\vartheta_l\right)} \quad (5)$$

where $\vartheta_e = T_e/T_F$ and $\vartheta_l = T_l/T_F$.

In eqs. (1) and (2), G is the electron-lattice coupling factor. A phenomenological temperature-dependent G suggested by Chen et al. [22] is adopted:

$$G = G_{RT}\left[\frac{A_e}{B_1}\left(T_e + T_l\right) + 1\right] \quad (6)$$

Since the electrons are more likely to collide with liquid atoms than the atoms in solid crystals, in the liquid phase, G, is taken to be 20% higher than that of the solid [23].

The laser irradiation is considered as a source term S in eq. (1):

$$S = \sum_{i=1}^{K}\sum_{j=1}^{N} \frac{0.94J_i(1-R)}{t_p(\delta+\delta_b)\left[1-e^{-L/(\delta+\delta_b)}\right]} \cdot \exp\left[-\frac{x}{(\delta+\delta_b)} - 2.77\left(\frac{t - \frac{i-1}{f_{rep}} - (j-1)t_{sep}}{t_p}\right)^2\right] \quad (7)$$

where K is the number of trains, N is the number of pulses in each train, t_{sep} is separation time between each single pulse, f_{rep} is the repetition rate, R is the reflectivity of the thin film, δ is the optical penetration depth, J is the laser pulse fluence, δ_b is the for the ballistic depth, and $[1-e^{-L/(\delta+\delta_b)}]$ is to correct the finite film thickness effect.

For a metal at its thermal equilibrium state, the thermal conductivity, k_{eq}, is the sum of the electron thermal conductivity, k_e, and the lattice thermal conductivity, k_l. In most cases k_e dominates k_{eq} because free electrons contribute to the majority part of heat conduction, For gold, k_l is usually taken to be 1% of k_{eq} [24], i.e.,

$$k_l = 0.01k_{eq} \quad (8)$$

A uniform temperature distribution is set to be the initial condition:

$$T_e\left(x, -2t_p\right) = T_l\left(x, -2t_p\right) = T_0 \quad (9)$$

Selecting $-2t_p$ as the initial time implies that the first laser pulse reaches its peak when $t = 0$.

On the right side of the film which receives laser irradiation, the heat loss caused by radiation will be considered while on the other side adiabatic boundary condition is applied:

$$\left.\frac{\partial T_e}{\partial x}\right|_{x=0} = \left.\frac{\partial T_e}{\partial x}\right|_{x=L} = \left.\frac{\partial T_l}{\partial x}\right|_{x=0} = 0 \quad (10)$$

$$\left.q_R''\right|_{x=L} = \sigma\varepsilon(T_{sur}^4 - T_\infty^4) \quad (11)$$

Before evaporation takes place, T_{sur} is the surface lattice temperature at $x = L$. After evaporation begins, T_{sur} is the liquid-vapor interface temperature which varies with the heating condition and needs to be determined.

The energy balance at the solid-liquid interface is described by [25]:

$$k_{l,s}\frac{\partial T_{l,s}}{\partial x} - k_{l,\ell}\frac{\partial T_{l,\ell}}{\partial x} = \rho_\ell h_m u_{s\ell} \qquad x = s(t) \quad (12)$$

where $T_{l,s}$ and $T_{l,\ell}$ are solid and liquid lattice temperature respectively, ρ is mass density, h_m is latent heat of fusion, and u_s is solid-liquid interfacial velocity. The additional interfacial velocity due to the density change during melting and resolidification has been considered.

For rapid melting and solidification processes, the velocity of the interface is dominated by nucleation dynamics, instead by the energy balance, eq. (12). For ultrashort-pulsed laser melting of gold, the velocity of the solid-liquid interface is described by [23]

$$u_{s\ell} = V_0\left[1 - \exp\left(-\frac{h_m}{R_g T_m}\frac{T_{l,I} - T_m}{T_{l,I}}\right)\right] \quad (13)$$

where V_0 is the maximum interface velocity, R_g is the gas constant for the metal, and $T_{l,I}$ is the interfacial temperature. The interfacial temperature, $T_{l,I}$, is higher than the normal melting point, T_m, during melting and lower than T_m during solidification.

Although the evaporation process is included in the current model, the simulation results show that within a wide range of parameters, the temperature will not exceed the boiling point. Therefore the introduction to the vaporization model is omitted here.

NUMERICAL MODEL

The governing equations (1) and (2) are discretized by the standard Finite Volume Method [26]. A fixed uniform grid with 2050 control volumes is adopted. The time step is variable in the numerical solution. The smallest time step is $10^{-2}t_p$, which is implemented during ($-2t_p$, $2t_p$) of each single pulse. The largest time step is $10^4 t_p$, which is implemented when the difference between electronic and lattice temperature is less than 1K.

In each time step, an iterative procedure will be employed to deal with the non-linear relationship between electron energy equation, lattice energy equation, solid-liquid and liquid-vapor interfaces. Electron energy equation (1) will be solved first using tri-diagonal matrix method (TDMA), then the lattice energy equation (2) will be solved. After obtaining an estimated electron and lattice temperature field, the velocity and temperature of solid-liquid interface will be obtained by using the method provided in Ref. [27] and is briefly described here:

(1) The solid-liquid interfacial temperature T_{sl} is assumed and the solid-liquid phase interfacial velocity is determined according to the interfacial energy balance;

(2) The interfacial velocity from the nucleation dynamics is obtained from Eq. (13);

(3) The interfacial velocities got from Steps (1) and (2) are compared. If the interfacial velocity obtained from the energy balance is higher than that from the nucleation dynamics, the interfacial temperature will be increased; otherwise, the interfacial temperature is decreased.

Steps 1-3 are repeated until the difference between the interfacial velocities obtained from the two methods is less than 10^{-5} m/s.

RESULTS AND DISCUSSION

1. Melting and resolidification of gold film with pulse train irradiation

First of all, the development of lattice temperature and solid-liquid interface during a typical irradiation process of a pulse train will be shown. The duration of each single pulse will remain constant as 100 fs and the thicknesses of the gold film for all cases are fixed at 1 μm. The initial temperature T_0, is set to be 300 K. The thermophysical and optical properties are given in Table 1.

At the repetition frequency of 1000 Hz, 10 pulse bursts irradiation with 3 single pulses in each burst separated by 100 ps will cause the evolution of surface lattice temperature as shown in Fig. 3. As can be seen in Fig. 3 (a), with each pulse burst depositing energy on the metal film, the temperature rises abruptly and drops rapidly. Figure 3(b) is the detailed temperature history for the eighth burst. In every burst, each single pulse will cause a peak in lattice temperature. After each peak, the temperature will fall with the conduction of heat into deeper part of the film. At the fifth burst, the lattice temperature exceeds the melting temperature (Fig. 3(a)), and the melting process will begin.

Table 1 Thermophysical and optical properties of gold

Coefficient for electronic heat capacity, B_e		70[2]
Material constant, A_e		1.2×10^7[22]
Material constant, B_1		1.23×10^{11}[22]
Electron-lattice coupling factor at room temperature, G_{RT} (W/m^3 K)	Solid	2.2×10^{16}[22]
	Liquid	2.6×10^{16}[22]
Specific heat, C_p (J/kg K)	Solid	$105.1+0.2941T_l-8.731\times10^{-4}T_l^2+1.787\times10^{-6}T_l^3-7.051\times10^{-10}T_l^4+1.538\times10^{-13}T_l^5$[15]
	Liquid	163.205[23]
Latent heat of evaporation at T_b, h_{lv} (J/kg)		1.698×10^6[28]
Latent heat of fusion, h_m (J/kg)		6.373×10^4[28]
Molar weight, M (kg/kmol)		196.967[28]
Reflection coefficient, R		0.6
Universal gas constant, R_u (J/K kmol)		8314.0
Boiling temperature, T_b (K)		3127
Critical temperature, T_c (K)		5590
Melting temperature, T_m (K)		1336
Fermi temperature, T_F (K)		6.42×10^4
Limit velocity , V_0 (m/s)		1300[23]
Coefficient for electronic conductivity, χ (W/m K)		353[21]
Optical penetration depth, δ (nm)		20.6
Ballistic range, δ_b (nm)		105[23]
Thermal conductivity at equilibrium, k_{eq} (W/m K)	Solid	$320.973-0.0111T_l-2.747\times10^{-5}T_l^2-4.048\times10^{-9}T_l^3$
	Liquid	$37.72+0.0711T_l-1.721\times10^{-5}T_l^2+1.064\times10^{-9}T_l^3$
Density, ρ (kg/m^3)	Solid	19.3×10^3
	Liquid	17.28×10^3

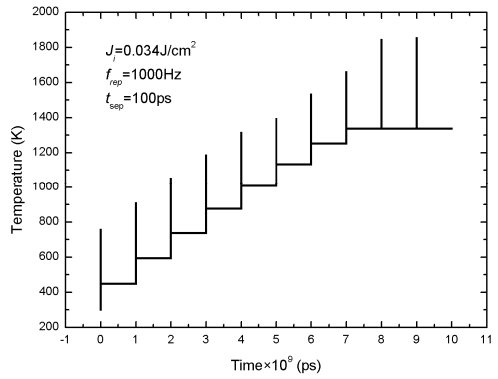

(a) Whole process

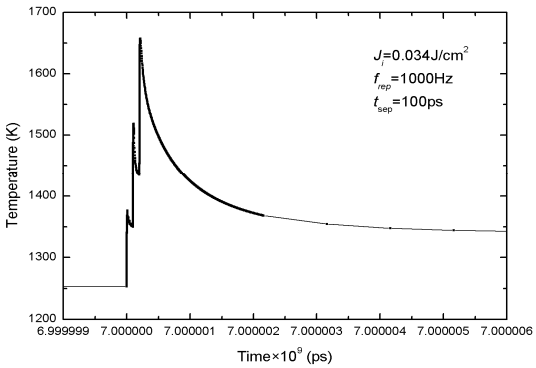

(b) During the 8th burst

Fig. 3 The surface lattice temperature caused by a typical laser pulse train

Figure 4 shows the evolution of the melting depth under the condition same as Fig. 3. It can be seen from Fig. 4(a) that after the fifth and sixth burst, resolidification will start and all the melted gold becomes solid state soon. This is because for pulse train irradiation, there is enough time for the heat to be transferred into the deeper part of the film. After the seventh burst, the melted gold solidifies very slowly. At this stage, the entire film is heated to be close to the melting point. All the incoming laser energy is used to provide the latent heat of melting.

2. Comparison with single pulse irradiation

To compare the result of pulse train with single pulse, five different single pulse fluences are used: 0.022, 0.026, 0.030, 0.034, and 0.036 J/cm^2. The other parameters are kept the same: repetition frequency 1000 Hz, separation time 100 ps, and 10 pulse bursts. The dependence of maximum lattice temperature and melting depth on the fluence is shown in Fig. 5. It is obvious that with higher laser fluence, deeper melting will be achieved and higher temperature will be caused. In the ultrafast laser materials processing, it is desirable that the melting depth can be accurately controlled and the temperature rise should be as low as possible to reduce the thermal stress.

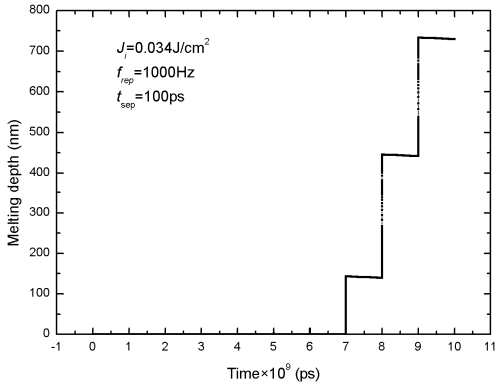

(a) Whole process

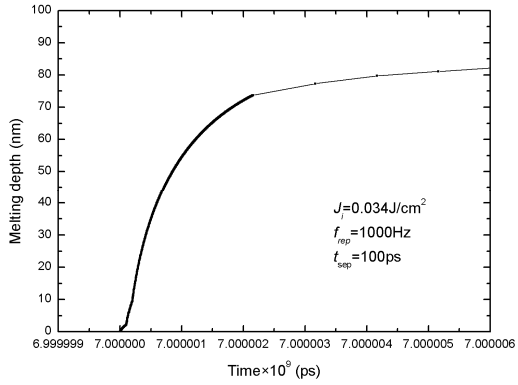

(b) During the 8th burst

Fig. 4 The evolution of melting caused by a typical laser pulse train

To compare the results of pulse train and single pulse irradiation, the relationship between the maximum lattice temperature and melting depth is shown in Fig. 6. The lower line is single pulse while the upper one is for pulse train. With the increase of pulse train power, the melting depth increases rapidly while the maximum lattice temperature increased relatively slowly. It is clear that with the same lattice temperature, the melting depth caused by pulse trains is much deeper than that caused by the single pulse. For example, the highest lattice temperature caused by a single 0.3 J/cm^2 pulse irradiation is almost the same as pulse trains which consists of 10 trains with 3 single 0.036 J/cm^2-pulses in a train, but its melting depth is only 50 nm, much less than the melting caused by the pulse train, almost 900 nm. On the other hand, to achieve the same melting depth, a pulse train will cause much lower lattice temperature, which is an advantage for laser-materials processing. However, it should also be noted that the energy needed for a pulse train is much higher that of a single pulse. According to Fig. 6, the melting depth caused by a single 0.3 J/cm^2 pulse is almost the same as the pulse train which consists of 10 bursts with 3 single 0.026-J/cm^2 pulses in a burst. But the total energy for the pulse train is 0.78J/cm^2. This is because more energy is used to heat up the deeper part of the film for the case of pulse train.

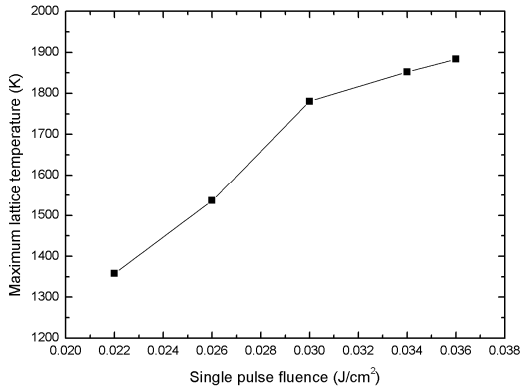

(a) Lattice temperature

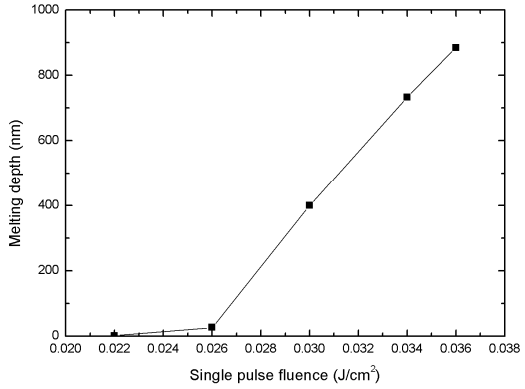

(b) Melting depth

Fig. 5 The effects of single pulse fluence on the irradiation process

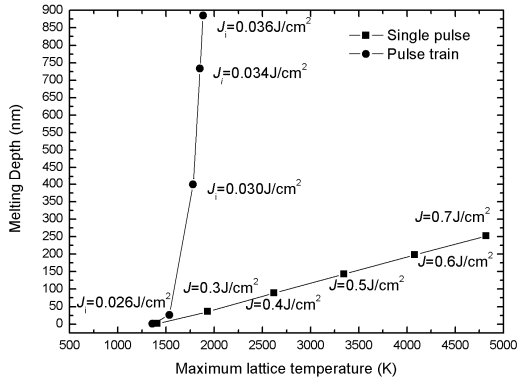

Fig. 6 The relationship between melting depth and maximum temperature, comparison between single pulse and pulse train

It should be noted that in Fig. 6 the lattice temperatures never reach 2000K, far blow the normal boiling point of gold, 3127 K. This is true for all the calculations in this paper. Before the lattice temperature reaches 3127 K, the whole film will be melted, at which point the calculation will stop.

From the above discussion, the merits of pulse train can be seen clearly. But to utilize laser pulse trains, there are much more parameters to be controlled than a single pulse irradiation did. The effects of parameters, including repetition rate, pulse numbers per train and separation time between single pulses will be studied below.

3. Repetition rate

Typical repetition rate for femtosecond lasers ranges from 100 Hz to tens of MHz. Numerical simulations are carried out for eight frequencies between 500 Hz and 1 MHz and different pulse fluence, and the results are shown in Fig. 7. Figure 7(a) shows the influence of repetition rate on the peak lattice temperature while Fig. 7(b) shows the effects on the melting depth. It is clear that repetition rate has little effects on the maximum temperature and the melting depth. This is because even for a high repetition rate as 1 MHz, there is still enough time between each train for the heat to transfer in the thin film and the melting depth will mainly be decided by the amount of energy deposited on the film.

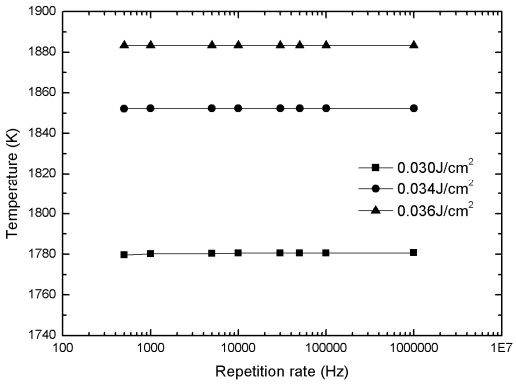

(a) Lattice temperature

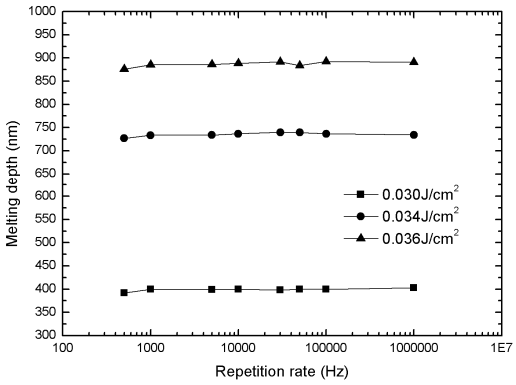

(b) Melting depth

Fig. 7 The effects of repetition rate

4. Pulse number per burst

Figure 8 shows the effect of pulse number in each burst while the total energy are kept at 0.09J/cm^2, 0.102J/cm^2, and 0.108J/cm^2 respectively. The repetition rate, separation time between single pulses and total burst number are kept at 10000 Hz, 100 ps and 10 respectively. Figure 8 (a) indicates that splitting laser pulse into more small pulses lowers the maximum temperature, but this effect weakens with the increase of pulse number per burst. Meanwhile, according to Fig. 8(b), the melting depth slightly increases with increasing number of pulse per burst.

5. Separation time

The separation time between two pulses in a burst is another important parameter. As stated in our earlier work [18], an appropriate separation time in multiple pulses irradiation will cause deeper melting and lower temperature.

Fig. 9 shows the effects of separation time on pulse train irradiation. The separation time ranges from 50~10000 ps. In Fig. 9 (a), it shows that with the increase of separation time, the maximum temperature is lowered. But when the separation time is larger than 5000 ps, the difference becomes very small. Figure 9(b) shows that in most cases longer separation time increases the melting depth but with small pulse fluence, it decreases the melting depth instead.

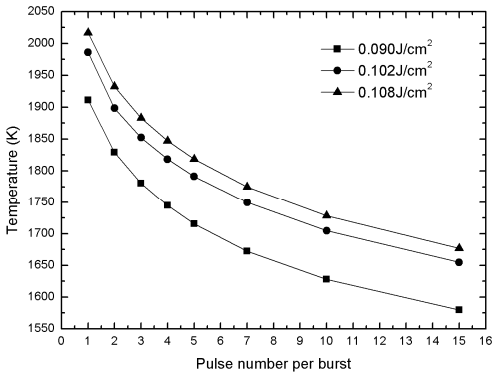

(a) Lattice temperature

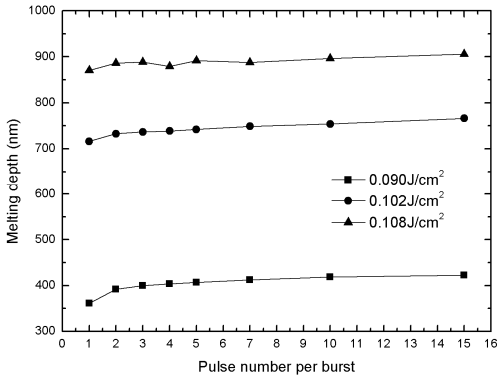

(b) Melting depth

Fig. 8 effects of pulse number per train

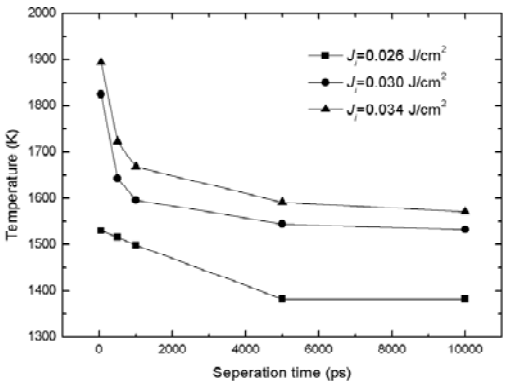

(a) Lattice temperature

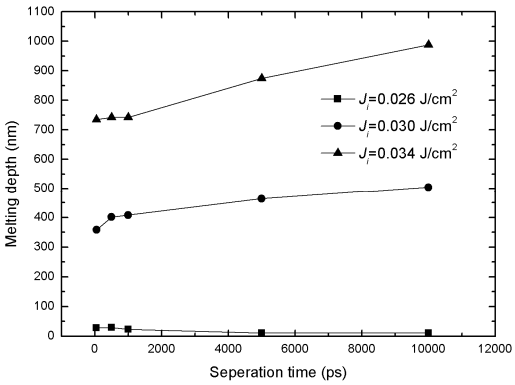

(b) Melting depth

Fig. 9 The effects of separation time between single pulses

6. Effects of boundary heat loss

In most computational study on laser metal interaction, the heat loss at boundaries was neglected, which is proved to be reasonable in our earlier work [17]. But for pulse train irradiation, the time scale is much larger in orders. The pulse train with a repetition rate of 1000 Hz has a time scale 10^{10} times larger than a typical 100-femtosecond laser pulse. Under this condition, the radiation caused heat loss may play a more important role in the process. Two computations were carried out: one with adiabatic boundary condition while another includes the radiation heat loss at the boundary. The results are shown in Fig. 10. The comparison between maximum lattice temperatures shows no obvious difference. But because the radiation at the surface will cause laser energy to escape from the film, the melting depth will be smaller than the results estimated by models ignoring this factor, as shown in Fig. 10(b). This means neglecting heat loss at surface will lead to an overestimation on melting depth when the repetition rate is low enough.

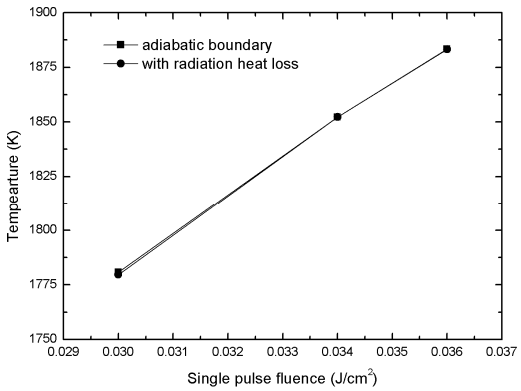

(a) Lattice temperature

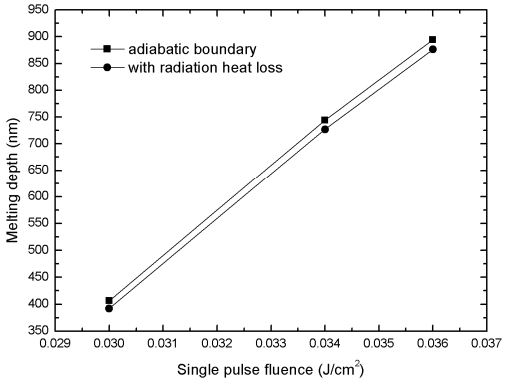

(b) Melting depth

Fig. 10 The effects of heat loss at surface

CONCLUSION

The interaction femtosecond laser pulse trains and a 1-μm free-standing gold film are simulated numerically. A two-temperature model coupled with interface tracking is employed to describe melting and resolidification processes during the irradiation. To deal with the large span in time scale, variable time steps are adopted. The laser beam consists of 10 pulse bursts with a repetition rate of 200~1000 Hz. Each pulse burst contains 3~10 single 100-fs laser pulses with an interval of 20~200 ps. The simulation results showed that:

(1) Compared to single-pulse irradiation, laser pulse train showed good performance in achieving deeper melting depth, especially in higher laser power. The temperature rise caused by laser irradiation increases relatively slowly with the increase of total laser energy deposited on the film;

(2) Repetition rate has little influence on the process. With the repetition rate ranges of 500 Hz to 1 MHz, the maximum lattice temperature and melting depth showed little change with all other parameters kept unchanged;

(3) By splitting a laser beam into many small single pulses, deeper melting depth and lower temperature will be achieved. Higher number of pulse per burst is preferable.

(4) With high laser power, the increase of separation time between single pulses will lead to lower temperature and deeper melting.

(5) With the repetition rate of 500 Hz, neglecting the heat loss caused by radiation on the surface may lead to an overestimation of melting depth.

ACKNOWLEDGMENTS

Support for this work by the U.S. National Science Foundation (NSF) under Grant No. CBET-0730143 and Chinese National Natural Science Foundation under Grant No. 50828601 is gratefully acknowledged.

REFERENCES

[1]. Anisimov, S. I., Kapeliovich, B. L., and Perel'man, T. L., 1974, "Electron emission from metal surfaces exposed to ultra-short laser pulses," Soviet Physics - JETP, 39(2): pp. 375-377.

[2]. Qiu, T. Q. and Tien, C. L., 1993, "Heat transfer mechanisms during Short-Pulse laser heating of metals," Journal of Heat Transfer, ASME, 115(4): pp. 835-841.

[3]. Tzou, D. Y., *Macro- to microscalse heat transfer*, 1997, Taylor & Francis: Washington, D.C.

[4]. Tzou, D. Y., *Computational techniques for Microscale heat transfer*, in Handbook of Numerical Heat Transfer, 2nd ed., W.J. Minkowycz, E.M. Sparrow, and J.Y. Murthy, Editors. 2006, Wiley, Hoboken, NJ.

[5]. Jiang, L. and Tsai, H. L., 2005, "Improved two-temperature model and its application in ultrashort laser heating of metal films," Journal of Heat Transfer, 127(10): pp. 1167-1173.

[6]. Chen, J. K., Tzou, D. Y., and Beraun, J. E., 2006, "A semiclassical two-temperature model for ultrafast laser heating," International Journal of Heat and Mass Transfer, 49(1-2): pp. 307-316.

[7]. Ivanov, D. S. and Zhigilei, L. V., 2007, "Kinetic limit of heterogeneous melting in metals," Physical Review Letters, 98(19): pp. 1957011-1957014.

[8]. Zhigilei, L. V., Ivanov, D. S., Leveugle, E., Sadigh, B., and Bringa, E. M., 2004, "Computer modeling of laser melting and spallation of metal targets," *Proceedings of SPIE Vol 5448*, SPIE.

[9]. Agarwala, M., Bourell, D., Beaman, J., Marcus, H., and Barlow, J., 1995, "Direct selective laser sintering of metals," Rapid Prototyping Journal, 1(1): pp. 26-36.

[10]. Ganesh, R. K., Faghri, A., and Hahn, Y., 1997, "A generalized thermal modeling for laser drilling process - I. Mathematical modeling and numerical methodology," International Journal of Heat and Mass Transfer, 40(14): pp. 3351-3360.

[11]. Shiomi, M., Yoshidome, A., Abe, F., and Osakada, K., 1999, "Finite element analysis of melting and solidifying

processes in laser rapid prototyping of metallic powders," International Journal of Machine Tools and Manufacture, 39(2): pp. 237-252.
[12]. Zacharia, T., David, S. A., Vitek, J. M., and Debroy, T., 1989, "Heat transfer during Nd: Yag pulsed laser welding and its effect on solidification structure of austenitic stainless steels," Metallurgical Transactions A, 20(5): pp. 957-967.
[13]. Zhang, Y., Faghri, A., Buckley, C. W., and Bergman, T. L., 2000, "Three-dimensional sintering of two-component metal powders with stationary and moving laser beams," Journal of Heat Transfer, 122(1): pp. 150-158.
[14]. Jiang, L. and Tsai, H. L., 2007, "Modeling of ultrashort laser pulse-train processing of metal thin films," International Journal of Heat and Mass Transfer, 50(17-18): pp. 3461-3470.
[15]. Jiang, L. and Tsai, H. L., 2006, "Energy transport and nanostructuring of dielectrics by femtosecond laser pulse trains," Journal of Heat Transfer, 128(9): pp. 926-933.
[16]. Zhang, Y. and Chen, J. K., 2007, "Melting and resolidification of gold film irradiated by nano- to femtosecond lasers," Applied Physics A: Materials Science and Processing, 88(2): pp. 289-297.
[17]. Huang, J., Zhang, Y. W., and Chen, J. K., 2009, "Ultrafast Solid-Liquid-Vapor Phase Change of a Gold Film Induced by Pico- to Femtosecond Lasers," Applied Physics A: Materials Science & Processing.
[18]. Huang, J., Zhang, Y. W., and Chen, J. K., 2009, "Ultrafast solid-liquid-vapor phase change in a thin gold film irradiated by multiple femtosecond laser pulses," International Journal of Heat and Mass Transfer.
[19]. Chen, J. K. and Beraun, J. E., 2004, "Superheating and material ablation of metals by multiple ultrashort laser pulses," Journal of Directed Energy, (1): pp. 93-109.
[20]. Chen, J. K. and Beraun, J. E., 2001, "Numerical study of ultrashort laser pulse interactions with metal films," Numerical Heat Transfer; Part A: Applications, 40(1): pp. 1-20.
[21]. Anisimov, S. I. and Rethfeld, B., 1997, "Theory of ultrashort laser pulse interaction with a metal," *Proceedings of SPIE Vol 3093*.
[22]. Chen, J. K., Latham, W. P., and Beraun, J. E., 2005, "The role of electron-phonon coupling in ultrafast laser heating," Journal of Laser Applications, 17(1): pp. 63-68.
[23]. Kuo, L. S. and Qiu, T. Q., 1996, "Microscale energy transfer during picosecond laser melting of metal films," *ASME National Heat Transfer Conference*.
[24]. Klemens, P. G. and Williams, R. K., 1986, "Thermal conductivity of metals and alloys," International metals reviews, 31(5): pp. 197-215.
[25]. Faghri, A. and Zhang, Y., *Transport phenomena in multiphase systems*, 2006, Elsevier Academic Press: Burlington, MA. 874.
[26]. Patankar, S., *Numerical Heat Transfer and Fluid Flow*, 1980, Taylor & Francis.
[27]. Zhang, Y. and Chen, J. K., 2008, "An interfacial tracking method for ultrashort pulse laser melting and resolidification of a thin metal film," Journal of Heat Transfer, 130(6): pp. 0624011-06240110.
[28]. Barin, I., *Thermochemical data of pure substance, Part I*, 1993, VCH: New York.